# Experimental Investigation of Nonlinear Fourier Transform Based Fibre Nonlinearity Characterisation

de Koster, P.B.J.; Koch, Jonas; Pachnicke, Stephan; Wahls, S.

# Experimental Investigation of Nonlinear Fourier Transform Based Fibre Nonlinearity Characterisation

Pascal de Koster[(1)], Jonas Koch[(2)], Stephan Pachnicke[(2)], Sander Wahls[(1)]

[(1)] Delft Center for Systems and Control, Delft University of Technology, p.b.j.dekoster@tudelft.nl
[(2)] Chair of Communications, Kiel University, jonas.koch@tf.uni-kiel.de

**Abstract**   *First experimental results on the characterisation of the nonlinear fibre coefficient using nonlinear Fourier transforms are reported for a 1000 km NZDSF fibre link. No special training signals were used. Instead, conventional pulse-shaped QPSK symbols were transmitted.*

## Introduction

Accurate knowledge of fibre parameters is essential for digital equalisation in fibre-optical communication systems, but full knowledge may not always be available in practice[1]–[5]. Classical fibre parameter estimation methods typically require special training signals[6]–[8], for which communication has to be interrupted or the modulation format has to be adapted. In earlier papers[9],[10], we proposed and validated (through simulations) a fibre identification method based on comparing the nonlinear Fourier spectra[11] of transmitted and received signals, to estimate a normalised model [see (4)–(5)] describing the propagation of the signal without any prior knowledge of the link. If the link length, number of spans, and loss coefficients are known, we can also recover the second-order dispersion and Kerr-nonlinearity coefficients. This method does not require special training signals and therefore has potential applications in the online monitoring of optical fibre links. The only requirement is that the transmitted signals are exciting the nonlinearity sufficiently.

In this paper, we present the first experimental results of nonlinear Fourier transform (NFT) based parameter estimation of a 1000 km link of non-zero dispersion shifted fibre (NZDSF) from regularly pulse-shaped QPSK transmission data.

The paper is structured as follows. We will first summarise the fibre model and the NFT. Next, we describe our experimental setup and the identification algorithm. Finally, we present the results and draw conclusions.

## Fibre model and nonlinear Fourier transform

Signal propagation in a span of single mode fibre with anomalous dispersion can be described by the nonlinear Schrödinger equation (NLSE)[12]:

$$A_l = -i\frac{\beta_2}{2}A_{\tau\tau} + i\gamma|A|^2 A - \frac{\alpha}{2}A, \qquad (1)$$

where $l$ is the position in the current fibre span, $\tau$ the time, $A(\tau,l)$ the signal envelope, $\beta_2 < 0$ the anomalous second-order dispersion coefficient, $\gamma > 0$ the Kerr-nonlinearity coefficient, and $\alpha$ the loss coefficient. Subscripts denote partial derivatives, and $i$ the imaginary unit. At the end of each fibre span of length $L_{\text{span}}$, the signal is amplified with lumped amplification, introducing ASE noise in the process.

To apply the NFT, we need a loss-free propagation model, which we obtain through the path-average approximation of a link with lumped amplification[13]:

$$Q = Ae^{-\alpha l/2}, \quad \gamma_1 = \gamma\frac{1 - e^{-\alpha L_{\text{span}}}}{\alpha L_{\text{span}}}, \qquad (2)$$

$$\Rightarrow Q_l \approx -i\frac{\beta_2}{2}Q_{\tau\tau} + i\gamma_1|Q|^2 Q. \qquad (3)$$

Here, $Q(\tau,l)$ is the loss-compensated amplitude, and $\gamma_1$ the path-average (PA) nonlinearity coefficient. To simplify the exposition of the NFT, the path-average NLSE is typically normalised[14]:

$$t = \tau, \quad q = \underbrace{\sqrt{|\gamma_1/\beta_2|}}_{c_q} Q, \quad z = \underbrace{-\beta_2/2}_{c_z} l \qquad (4)$$

$$\Rightarrow q_z = iq_{tt} + 2i|q|^2 q, \qquad (5)$$

with $q(t,z)$ the normalised signal envelope, $c_q$ the amplitude normalisation coefficient and $c_z$ the space normalisation coefficient.

The NFT of a signal $q(t) = q(t,z_0)$ with vanishing boundary conditions is defined through the
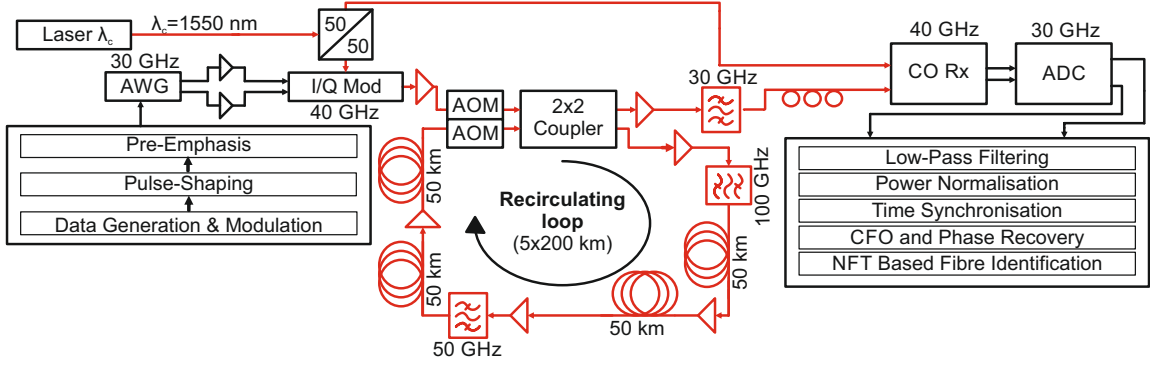
**Fig. 1:** The experimental setup, with the transmitter at the left, the 1000 km NZDSF link in the middle, and the receiver at the right. Acronyms: AWG: arbitrary waveform generator; AOM: acousto optic modulator; CFO: carrier frequency offset.

Zahkarov-Shabat scattering problem[11],[15]:

$$\frac{d}{dt}\begin{bmatrix} \phi_1(t,\lambda) \\ \phi_2(t,\lambda) \end{bmatrix} = \begin{bmatrix} -i\lambda & q(t) \\ -q^*(t) & i\lambda \end{bmatrix}\begin{bmatrix} \phi_1(t,\lambda) \\ \phi_2(t,\lambda) \end{bmatrix},$$

$$\begin{bmatrix} e^{-i\lambda t} \\ 0 \end{bmatrix} \underset{t\to-\infty}{\longleftarrow} \begin{bmatrix} \phi_1(t,\lambda) \\ \phi_2(t,\lambda) \end{bmatrix} \underset{t\to+\infty}{\longrightarrow} \begin{bmatrix} a(\lambda)e^{-i\lambda t} \\ b(\lambda)e^{+i\lambda t} \end{bmatrix}, \quad (6)$$

in which $\lambda$ is the nonlinear frequency, $\phi$ the eigenfunction, and $(\cdot)^*$ complex conjugation. The eigenfunction is fixed in the left far-field. The resulting behaviour in the right far-field defines the scattering coefficients $a(\lambda)$ and $b(\lambda)$. The NFT finally consists of a continuous spectrum $\{b(\lambda) : \lambda \in \mathbb{R}\}$, and a discrete spectrum $\{\lambda_k : a(\lambda_k) = 0, \Im(\lambda_k) > 0\}$. When a signal propagates according to the normalised NLSE, the amplitudes of the continuous spectrum and the eigenvalues of the discrete spectrum remain constant[15].

**Experimental setup and data processing**

The experimental setup is depicted in Fig. 1. 100 bursts of 128 QPSK symbols with a symbol-rate of 10 GBd (burst length 12.8 ns) were transmitted with a guard interval in between bursts. For pulse-shaping a root-raised cosine filter with roll-off factor of 0.5 was used. This was followed by a pre-emphasis to compensate for the imperfections of the electrical components. Digital to analogue conversion was done using an 88 GS/s AWG. The analogue signal was converted into the optical domain using an I/Q modulator and a laser with 1 kHz linewidth. The optical signal was fed into a recirculating loop consisting of four spans of 50 km True-Wave NZDSF ($D \approx 4.5\frac{\text{ps}}{\text{nm·km}}, \gamma \approx 1.6\frac{1}{\text{W·km}}, \alpha \approx 0.22\frac{\text{dB}}{\text{km}}$) with a launch-power of 0 dBm. After polarisation de-rotation using a manual polarisation controller the signal was detected by a coherent receiver using the transmitter laser as local oscillator and subsequently analogue to digital converted (80 GS/s). The frequency response of the back-to-back sys-

tem was measured once. For the analysis, this frequency response was used to filter the digital input signal. The received signal was filtered, power normalised, time synchronised, and frequency and phase synchronised. The NFT was determined with the software library *FNFT*[16], using initial guesses for the eigenvalues obtained through Fourier collocation[17].

**Fibre identification algorithm**

In this section, we describe and adjust the relevant parts of the NFT-based fibre identification algorithm[10]. In our previous work, the algorithm was only tested in simulations. Out of the box, applying the algorithm to experimental data did not provide accurate enough estimates of $c_z = -\beta_2/2$ due to additional distortions in the $b$-coefficients. Thus, we instead estimated $\beta_2$ classically by comparing the phases of the linear Fourier transforms of the received and transmitted signals. Only $c_q$ is estimated using NFTs in this first experimental demonstration. An improved version of the algorithm will be investigated in future work.

Following the original algorithm[10], we identify $c_q$ by comparing NFT eigenvalues from received and transmitted signals, while $c_q$ is varied. At the correct normalisation constant $c_q = c_q^{\text{PA}}$ with respect to the path-average model, the input and output eigenvalues should match optimally. The error is defined by creating a minimum-cost matching between input- and output-eigenvalues. We define a full bipartite graph with the input eigenvalues on one side, and the output eigenvalues on the other side, and set each edge cost $E_{km}$ to the Euclidean distance between the eigenvalues, but limited by their sum of imaginary parts:

$$E_{km} = \min\left(|\lambda_m^{\text{out}} - \lambda_k^{\text{in}}|, \Im(\lambda_k^{\text{in}} + \lambda_m^{\text{out}})\right). \quad (7)$$

The limit ensures that eigenvalues with small imaginary part (proportional to energy[14]) cannot dominate the error. The error of an unmatched
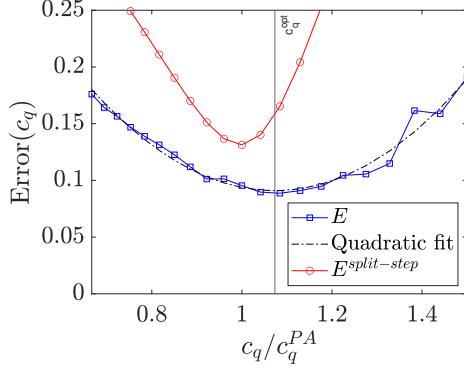
**Fig. 2:** The matching error vs. $c_q$ for a single signal of 128 symbols. The $L_1$-error between the received signal and the numerically split-step forward propagated transmitted signal is also shown for comparison.

eigenvalue is set equal to its imaginary part.

Finally, the total error is the least-cost matching, where $m(k)$ denotes the matching connecting $\lambda_k^{\text{in}}$ to $\lambda_m^{\text{out}}$. The error is normalised by the sum of imaginary parts of all eigenvalues:

$$E = \min_{m(k)} \frac{\sum_k E_{km(k)}}{\sum_k \Im\left(\lambda_k^{\text{in}}\right) + \sum_m \Im\left(\lambda_m^{\text{out}}\right)}. \qquad (8)$$

We determined the minimum-cost matching $m(k)$ with a fast version of the Hungarian algorithm[18].

**Results**

We applied the algorithm to the experimental data. For each of the bursts, we swept $c_q$ from 67% to 150% of the expected normalisation $c_q^{\text{PA}}$ according to the path-average model of Eq. 2 and Eq. 4. The expected normalisation $c_q^{\text{PA}}$ was determined using $\beta_2 = -5.48\frac{\text{ps}^2}{\text{km}}$ ($D = 4.3\frac{\text{ps}}{\text{nm}\cdot\text{km}}$) measured with linear FFT, and $\gamma = 1.6\frac{1}{\text{W}\cdot\text{km}}$ as indicated by the data sheet of the fibre. We determined the optimal $c_q$ by fitting a parabola to the error, and locating its minimum, as shown in Fig. 2 for one of the bursts. Due to the many local minima of the error function, this method is usually more reliable and faster than performing local minimisation. The $L_1$-error between the received signal and the numerically forward-propagated transmitted signal is also shown for various $c_q$, which confirms that the nonlinearity coefficient from the data sheet indeed describes the fibre well. Fig. 3 shows the spectral matching for the optimal $c_q$ of the same burst as in Fig. 2. We observed that the difference in eigenvalues is significantly larger for our experimental data than for comparable simulation data with a similar noise profile. This indicates that transceiver impairments play a significant role.

Fig. 4 shows the identified normalisation $c_q$ from all 100 bursts, compared to the $\beta_2$ and $c_q^{\text{PA}}$
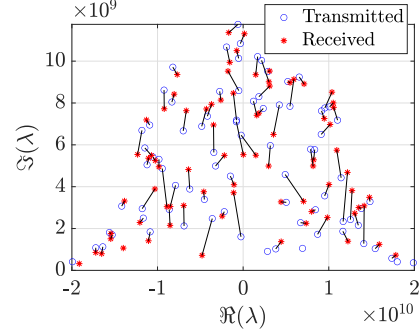


**Fig. 3:** The matching of discrete spectra at optimal normalisation of one of the signals.
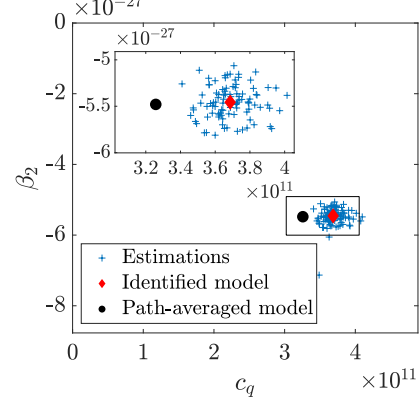


**Fig. 4:** The estimated fibre model: blue crosses mark the 100 estimations from each individual burst; the red diamond marks the average of all estimations. The black dot marks the expected model according to path-averaging.

expected from the True-Wave NZDSF. The measured $\beta_2$ coefficient was 5% smaller than the value derived from the data sheet, and the identified normalisation coefficient $c_q$ was about 13% higher. The estimated $\gamma_{\text{est}}$ of our algorithm is $2.0\frac{1}{\text{W}\cdot\text{km}}$, which is higher than the value of the data sheet ($1.6\frac{1}{\text{W}\cdot\text{km}}$). This first validation nevertheless shows that the proposed method can at least coarsely identify the normalisation coefficient, and in turn the fibre parameters. Although this estimate is not yet as close as the split-step based method, keep in mind that the $b$-coefficients were not used at the moment due to additional distortions. We expect that better results can be obtained by improving the $b$-related parts of the algorithm[10], as well as by improving the data pre-processing.

**Conclusion**

We have investigated a nonlinear Fourier transform based fibre identification technique on experimental data. Using only the eigenvalues of the nonlinear Fourier spectrum, we were able to get a coarse estimate of the Kerr nonlinearity parameter. Future research will focus on including the full nonlinear spectrum for experimental data to improve the accuracy of the estimates.

## References

[1] F. N. Hauske, C. Xie, Z. Zhang, C. Li, L. Li, and Q. Xiong, "Frequency domain chromatic dispersion estimation", in *2010 Conference on Optical Fiber Communication (OFC/NFOEC), collocated National Fiber Optic Engineers Conference*, IEEE, 2010, pp. 1–3.

[2] Q. Sui, A. P. T. Lau, and C. Lu, "Fast and robust blind chromatic dispersion estimation using auto-correlation of signal power waveform for digital coherent systems", *Journal of Lightwave Technology*, vol. 31, no. 2, pp. 306–312, 2013.

[3] C.-Y. Lin, A. Napoli, B. Spinnler, V. Sleiffer, D. Rafique, M. Kuschnerov, M. Bohn, and B. Schmauss, "Adaptive digital back-propagation for optical communication systems", in *Optical Fiber Communication Conference*, Optical Society of America, 2014, pp. M3C–4.

[4] M. Piels, E. P. da Silva, D. Zibar, and R. Borkowski, "Performance emulation and parameter estimation for nonlinear fibre-optic links", in *2016 21st European Conference on Networks and Optical Communications (NOC)*, IEEE, 2016, pp. 1–5.

[5] L. Jiang, L. Yan, A. Yi, Y. Pan, M. Hao, W. Pan, B. Luo, and Y. Jaouën, "Chromatic dispersion, nonlinear parameter, and modulation format monitoring based on godard's error for coherent optical transmission systems", *IEEE Photonics Journal*, vol. 10, no. 1, pp. 1–12, 2018.

[6] Y. Namihira, A. Miyata, and N. Tanahashi, "Nonlinear coefficient measurements for dispersion shifted fibres using self-phase modulation method at 1.55 µm", *Electronics Letters*, vol. 30, no. 14, pp. 1171–1172, 1994.

[7] A. Boskovic, S. Chernikov, J. Taylor, L. Gruner-Nielsen, and O. Levring, "Direct continuous-wave measurement of $n_2$ in various types of telecommunication fiber at 1.55 µm", *Optics letters*, vol. 21, no. 24, pp. 1966–1968, 1996.

[8] P. André and J. Pinto, "Simultaneous measurement of the nonlinear refractive index and chromatic dispersion of optical fibers by four-wave mixing", *Microwave and Optical Technology Letters*, vol. 34, no. 4, pp. 305–307, 2002.

[9] P. de Koster and S. Wahls, "Fibre model identification for nonlinear Fourier transform-based transmission", in *45th European Conference on Optical Communication (ECOC 2019)*, IET, 2019, pp. 1–4.

[10] P. de Koster and S. Wahls, "Dispersion and nonlinearity identification for single-mode fibers using the nonlinear Fourier transform", *Journal of Lightwave Technology*, 2020.

[11] M. J. Ablowitz, D. J. Kaup, A. C. Newell, and H. Segur, "The inverse scattering transform-Fourier analysis for nonlinear problems", *Studies in Applied Mathematics*, vol. 53, no. 4, pp. 249–315, 1974.

[12] G. P. Agrawal, *Fiber-optic communication systems*. John Wiley & Sons, 2012, vol. 222.

[13] S. T. Le, J. E. Prilepsky, and S. K. Turitsyn, "Nonlinear inverse synthesis technique for optical links with lumped amplification", *Optics express*, vol. 23, no. 7, pp. 8317–8328, 2015.

[14] M. I. Yousefi and F. R. Kschischang, "Information transmission using the nonlinear Fourier transform, part I: Mathematical tools", *IEEE Transactions on Information Theory*, vol. 60, no. 7, pp. 4312–4328, 2014.

[15] A. Shabat and V. Zakharov, "Exact theory of two-dimensional self-focusing and one-dimensional self-modulation of waves in nonlinear media", *Soviet physics JETP*, vol. 34, no. 1, p. 62, 1972.

[16] S. Wahls, S. Chimmalgi, and P. J. Prins, "FNFT: A software library for computing nonlinear Fourier transforms", *Journal of Open Source Software*, vol. 3, no. 23, p. 597, 2018.

[17] F. J. García-Gómez and V. Aref, "Statistics of the nonlinear discrete spectrum of a noisy pulse", *Journal of Lightwave Technology*, vol. 37, no. 14, pp. 3563–3570, 2019.

[18] H. W. Kuhn, "The Hungarian method for the assignment problem", *Naval research logistics quarterly*, vol. 2, no. 1-2, pp. 83–97, 1955.